PCCP

ELECTRONIC SUPPLEMENTARY INFORMATION

Hidden negative linear compressibility in lithium L-tartrate

H. H.-M. Yeung, R. Kilmurray, C. L. Hobday, S. C. McKellar, A. K. Cheetham, D. R. Allan and S. A. Moggach

S1. Detailed Experimental Section

Synthetic procedure.

All chemical reagents were used as-received: l-tartaric acid (≥98 %, Sigma-Aldrich), lithium acetate dihydrate (98 %, Fisher Scientific U.K.), ethanol (reagent grade, Fisher Scientific U.K.) and in-house deionized water. l-tartaric acid (1 mmol) and lithium acetate dihydrate (2 mmol) were placed in a stainless steel autoclave with PTFE-liner in the reaction tubes with minimal mixing, followed by water:ethanol (1:2, 10 mL). The autoclave was sealed tightly and placed in an oven at 150 °C for one week, before being allowed to cool to room temperature and opened, yielding large slab-shaped single crystals of **1**.

Variable-pressure crystallography.

High-pressure experiments were carried out using a modified Merrill-Bassett diamond anvil cell (DAC) equipped with 600 μm culet diamonds and a tungsten gasket.[1] A single-crystal of in lithium L-tartrate (Li_2(L-$C_4H_4O_6$), denoted **1** in the text) and a chip of ruby were loaded into the DAC with a 4:1 by volume mixture of methanol:ethanol as a hydrostatic media. The pressure inside the DAC was measured using the ruby fluorescence method.[2]

A sphere of data were collected for a single-crystal of Li_2(L-$C_4H_4O_6$) at ambient pressure and temperature. The data were collected on a Bruker SMART APEXII diffractometer using graphite monochromated Mo Kα radiation (λ = 0.71073 Å). These data were used as a reference for the high-pressure data which were also collected at ambient temperature. The data were integrated using the program SAINT, and the absorption correction was carried out using the program SADABS.[3] All of the obtained data were refined against F^2 using CRYSTALS.[4] The structure was refined anisotropically against F^2. H-atoms attached to C-atoms were placed geometrically, while the hydroxyl H-atoms were found in a difference map, and refined. A distance restraint (O-H = 0.84, 0.01) was applied to the hydroxyl H-atoms.

Laboratory high-pressure diffraction data were collected on the same crystal on a Bruker SMART APEXII diffractometer using graphite monochromated Mo Kα radiation (λ = 0.71073 Å). Data were collected in ω-scans in twelve settings of 2θ and φ with a frame time and step size of one second and 0.3º respectively. This collection strategy was based on that described by Dawson *et al.*[5] In a similar method to the ambient data, the high pressure data were integrated using the program SAINT.[6] In order to prevent the integration of regions in the diffraction pattern that had been shaded by the pressure cell, 'dynamic masks' were used. The absorption correction was carried out using the programs SHADE[7] and SADABS[3] to correct for adsorption from the pressure cell and sample, respectively. Data were collected from 0.14 up to 4.00 GPa, however, only the data collected from sample pressures of 0.14, 0.68, 1.12 and 2.59 GPa were used in the analysis of this experiment. This is because the sample had become dislodged in the DAC and at these 4 pressures minimal sample movement was observed, and the data could be processed.

In order to obtain better data to higher pressures, a second crystal of Li_2(L-$C_4H_4O_6$) was loaded inside a DAC and diffraction data collected on station I19 at the DIAMOND Light Source, Rutherford Appleton Laboratory, with a Rigaku Saturn 724 CCD detector using synchrotron radiation (λ = 0.5159 Å). Data collections were carried out using an exposure time and a step size of 1 second and 0.5 degrees respectively. The data were integrated using the programme SAINT using dynamic masks, these mask the regions of the detector which are shaded due to the pressure cell.[6] Omission of shaded reflections, absorption correction and merging of data were carried out in a three-step process, firstly with the programme SHADE,[7] then SADABS[3] and finally XPREP.[8]

High pressure structure refinements were carried out in CRYSTALS.[4] Non-hydrogen atoms were refined isotopically against F^2 for all laboratory and synchrotron high-pressure date. All 1,2 and 1,3 distances for the L-tartrate were restrained, whilst all torsion angles and Li-O bond distances were allowed to freely refine. Vibrational and thermal similarity restraints were also applied. H-atoms attached to C-

atoms were placed geometrically, while the hydroxyl H-atoms were found in a difference map, and refined for the synchrotron data. Once converged, these were then constrained to ride on the parent O-atom.

Variable-temperature crystallography.

X-ray diffraction was performed on an Oxford Diffraction Gemini E Ultra diffractometer using Mo radiation (λ = 0.7107 Å, operating at 50 kV and 40 mA). Data were collected at intervals of 10 K from 120 K to 490 K using ω scans. An Eos CCD plate detector was used with mean detector area resolution 16.1 pixels mm^{-1}. Data collection, cell determination, transformation and refinement, intensity integration and face indexation were performed using CrysAlisPro software.[9] Structures were solved by direct methods and full matrix least-squares refinements against $|F^2|$ were carried out using the OLEX2 programme.[10] All non-hydrogen atoms were refined anisotropically; hydrogen atoms were then inserted using a riding model and refined with isotropic displacement parameters constrained to 1.2 and 1.5 times those of their adjacent carbon (non-methyl), and oxygen and methyl carbon atoms, respectively. Where the automatic choice of monoclinic cell produced a setting different to the original ambient temperature/pressure one, it was transformed using the matrix [1 0 -1 0 -1 0 0 0 -1] to produce the same setting as original.

S2. Crystal structure and properties

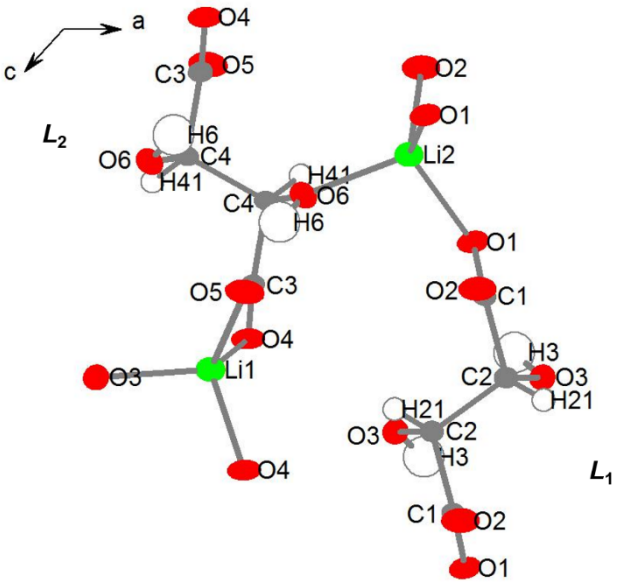

Figure S1. Extended asymmetric unit of lithium L-tartrate, **1**, viewed approximately down the *b*-axis, showing C, H, Li and O atoms in grey, white, green and red, respectively. Crystallographically distinct ligands are labelled L1 and L2 as described in the main text.

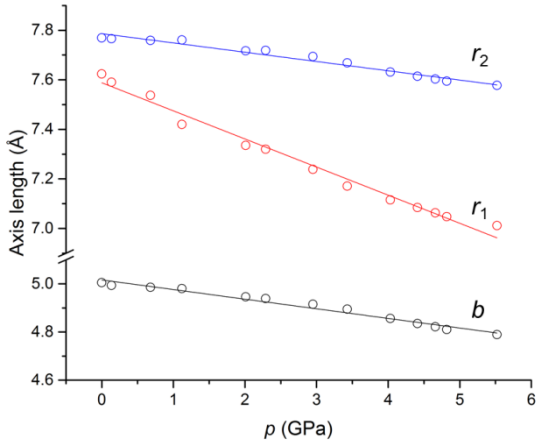

Figure S2. Variation of unit cell parameter *b* and wine-rack strut lengths r_1 and r_2 as a function of pressure, showing linear fits used to determine linear compressibilities.

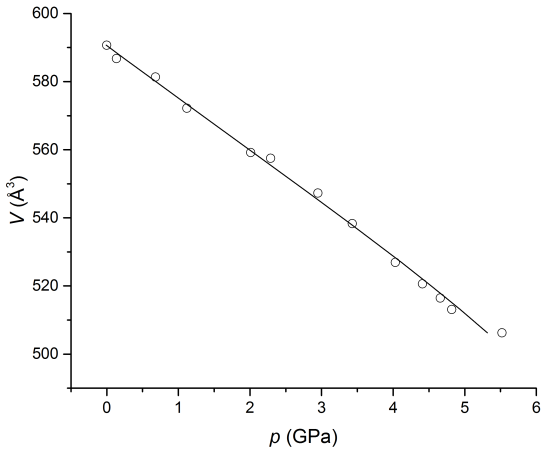

Figure S3. Variation of unit cell volume, V, as a function of pressure, p, showing the third-order Birch-Murnaghan fit used to determine bulk modulus, B_0.

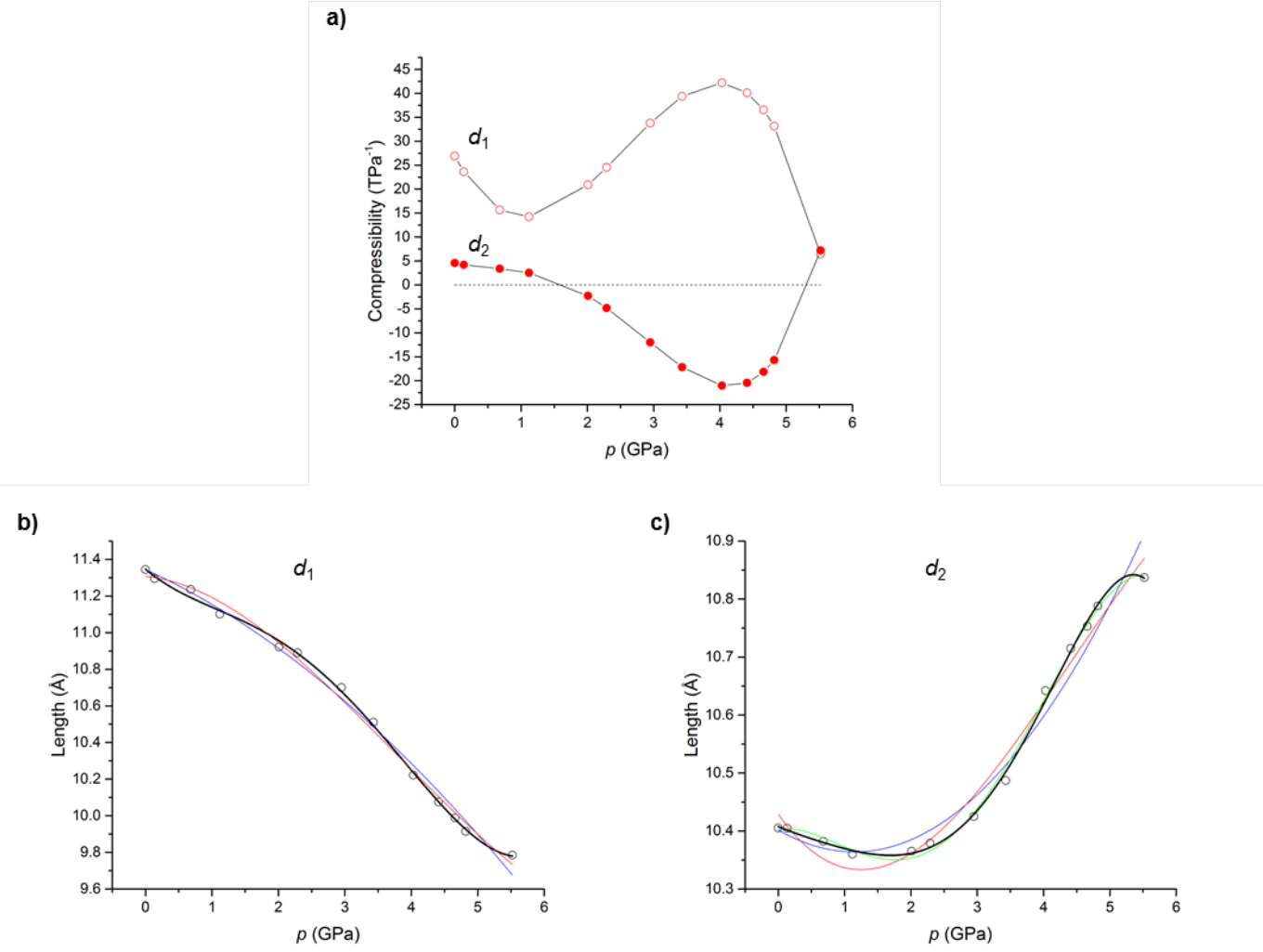

Figure S4. Pressure-dependent compressibility of wine-rack diagonal vectors d_1 and d_2 (a), calculated from polynomial fits to the data (b and c). The polynomial functions selected for calculation of compressibilities (4th and 5th-order, respectively) are shown as thick black lines, whilst less satisfactory fits are shown in blue (2nd order), red (3rd order) and green (4th order). Whilst the absolute values of compressibility at ambient pressure can be seen to depend considerably on the polynomial order used, the behaviour at elevated pressures, particularly through the PLC-NLC transition, is well modelled by the selected functions.

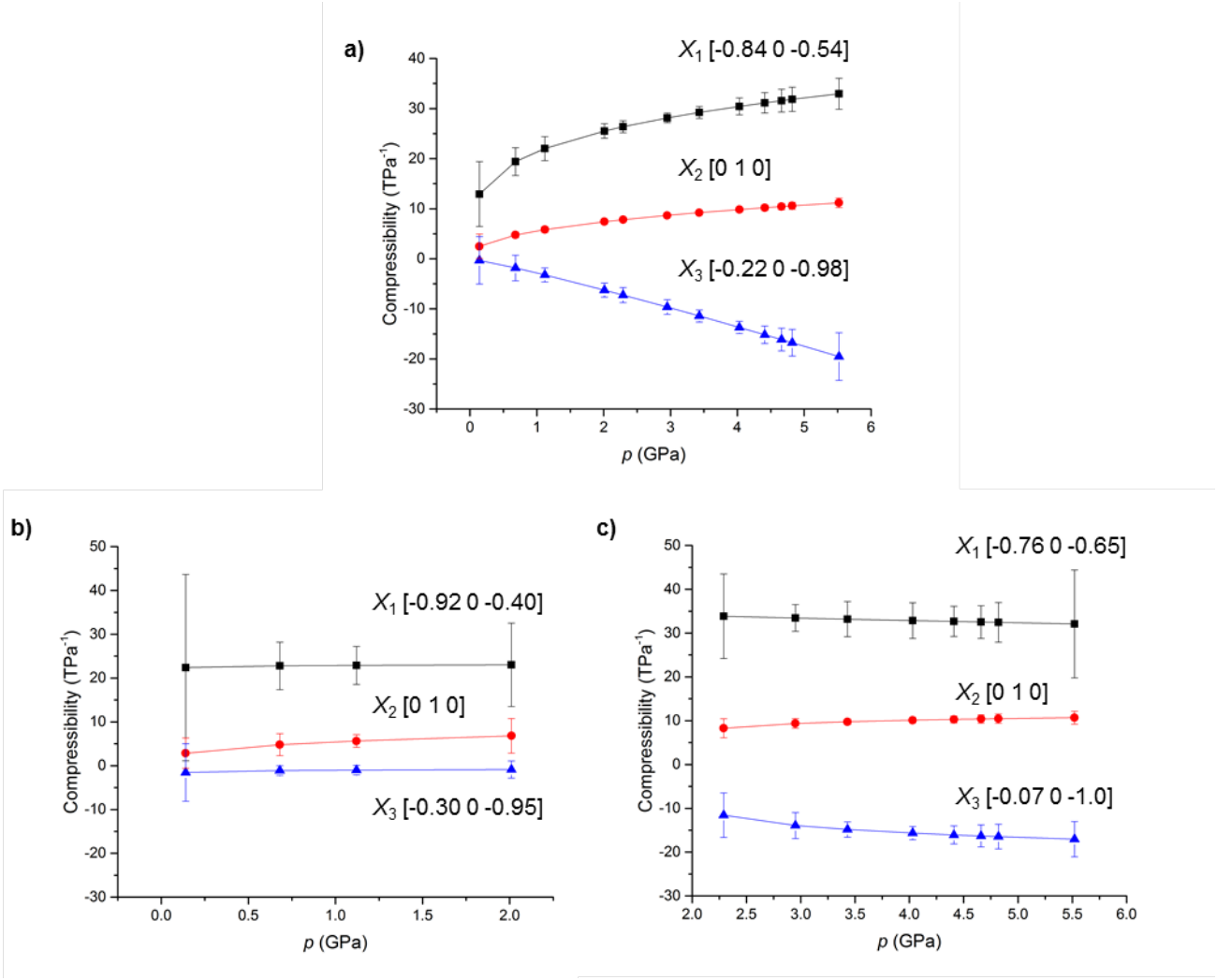

Figure S5. Linear compressibilities, *K*, vs. hydrostatic pressure, *p*, showing directions of principle axes, *X*, calculated using PASCal[12] for a) all data, b) data below 2 GPa, and c) data above 2 GPa.

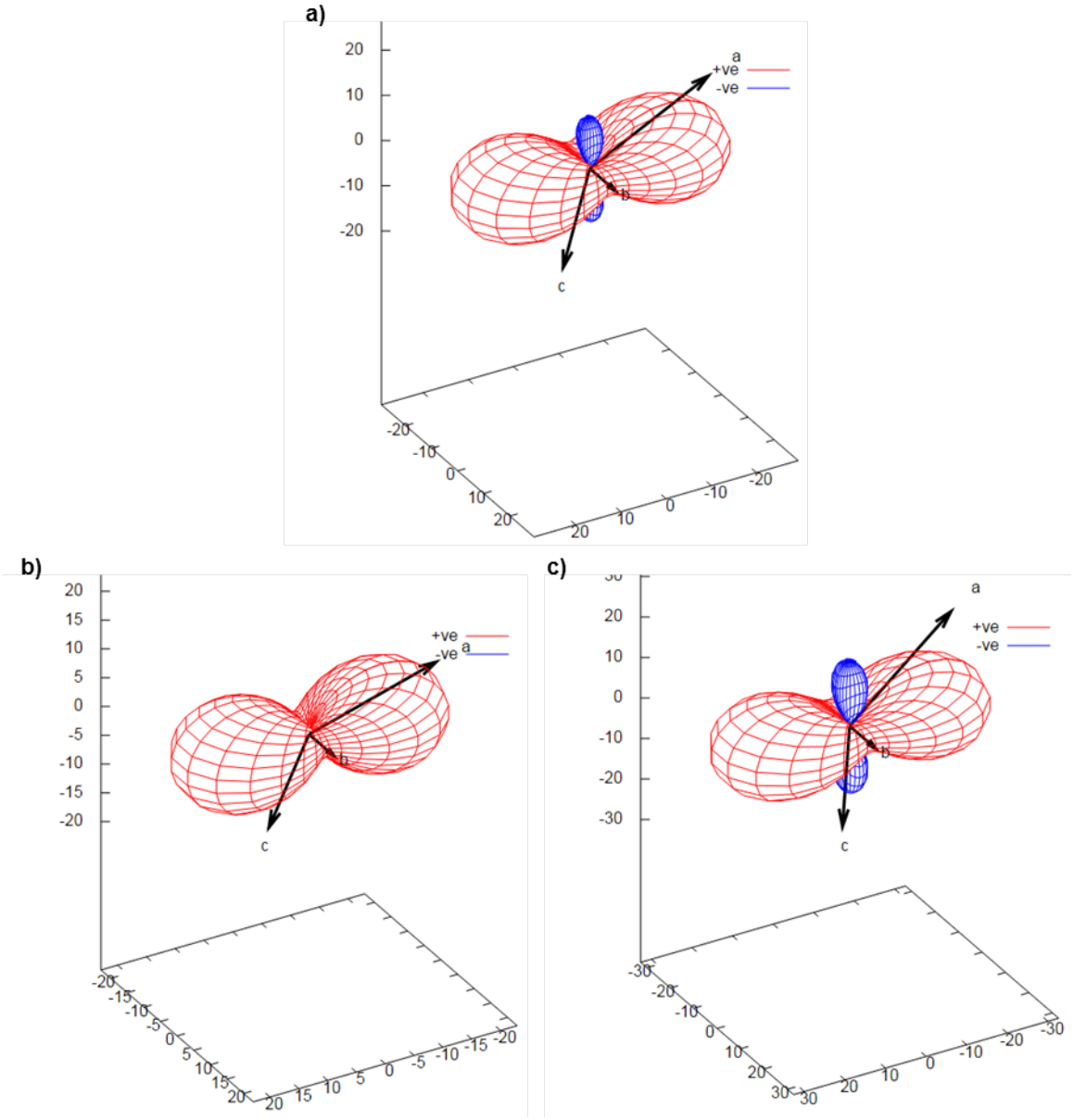

Figure S6. Linear compressibility indicatrices of **1**, calculated using PASCal[12] for a) all data, b) data below 2 GPa, and c) data above 2 GPa. Blue = negative, red = positive compressibility; all axes in units of TPa^{-1}.

Wine-rack axis	K / TPa^{-1}	Direction
i) Ambient pressure limit		
d_1	26.9	[1 0 1]
b	8.0	[0 1 0]
d_2	4.6	[0 0 1]
ii) 4.0 GPa		
d_1	42.2	[1 0 1]
b	8.2	[0 1 0]
d_2	-21.0	[0 0 1]

Principle axis	K / TPa^{-1}	[100] component	[010] component	[001] component
iii) 0-2.0 GPa region				
X_1	23(4)	0.9162	0	0.4007
X_2	5.6(14)	0	1	0
X_3	-1.0(11)	0.3007	0	0.9537
iv) 2.0-5.5 GPa region				
X_1	33(3)	0.7567	0	0.6537
X_2	10.3(8)	0	1	0
X_3	-16(2)	0.07	0	0.9975
v) 0-5.5 GPa region				
X1	29.2(12)	0.8428	0	0.5382
X2	9.2(3)	0	1	0
X3	-11.4(12)	0.2193	0	0.9757

Table S1. **L**inear compressibilities, K, for wine-rack axes (calculated by polynomial fits) in i) the ambient pressure limit, and ii) at 4.0 GPa. Axes of principle strain (median compressibilities and directionalities) calculated using the PASCal program[12] are shown for comparison in iii) the pressure range 0-2 GPa, iv) above 2 GPa, and v) for all data.

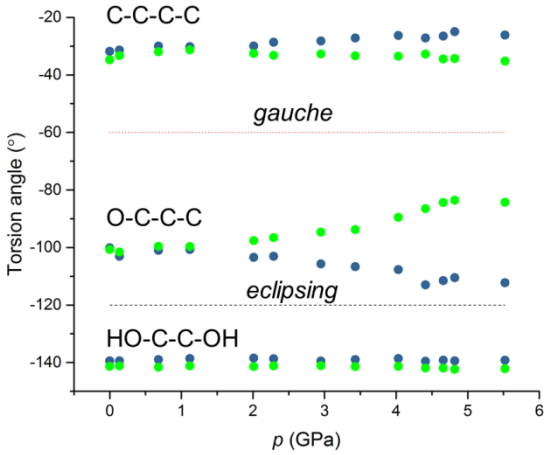

Figure S7. Pressure-dependent variation of the torsion angles of the tartrate ligands L1 (blue/grey) and L2 (lime green). Dotted lines mark the angles of *gauche* and *eclipsing* interactions.

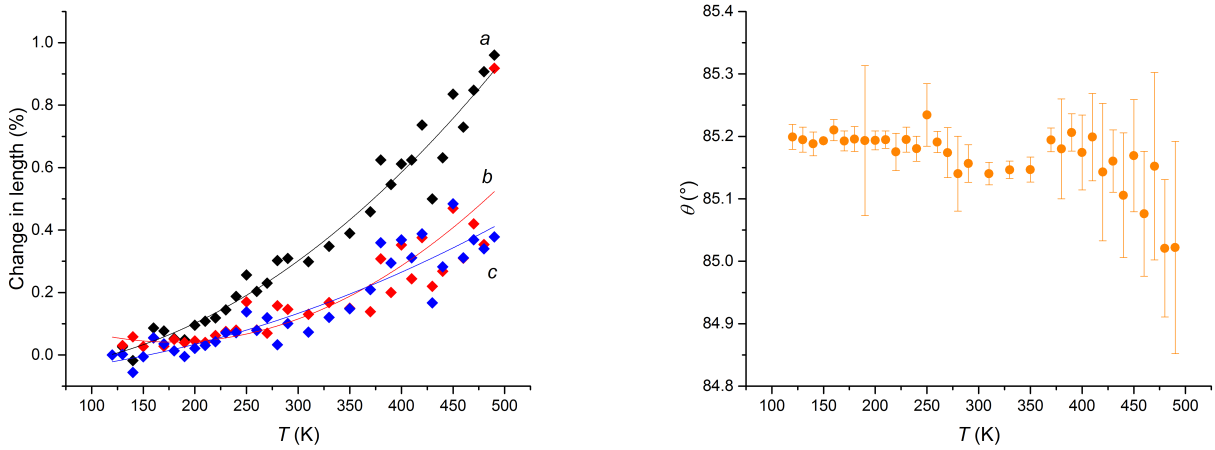

Figure S8. Relative changes in unit cell parameters of **1** with temperature, measured by single crystal X-ray diffraction. a) Unit cell lengths, fitted by 2nd order polynomial functions; b) wine-rack angle, θ.

Wine-rack axis	K / TPa^{-1}	Principle axis	K / TPa^{-1}	[100]	[010]	[001]
i) 0 GPa limit		0 – 2.0 GPa region.				
d_1 [101]	26.9	X_1	23(4)	0.9162	0	0.4007
b [010]	8.0	X_2	5.6(14)	0	1	0
d_2 [001]	4.6	X_3	-1.0(11)	0.3007	0	0.9537
Wine-rack axis[a]	α / MK^{-1}	Principle axis	α / MK^{-1}	[100]	[010]	[001]
ii) 120 K – 490 K variable temperature						
d_1 [101]	16.4(11)					
b [010]	7.1(7)	X_2	13(2)	0	1	0
d_2 [001]	11.7(9)	X_1	3.7(9)	0.388	0	0.9217
r_1 [100]	24.7(11)	X_3	24.6(12)	0.9915	0	0.13
r_2	4.3(10)					

Table S2. i) Low pressure compressibility and ii) coefficients of linear and volume thermal expansion of **1**, α, and directions for the range 120 – 490 K, calculated using the PASCal program.[12] [a]relation to the crystallographic unit cell is $r_2 = \sqrt{\left(\left(a/2\right)^2 + c^2 + a.c.\cos\beta\right)}$.

S3. Crystal structure refinements

Table S3. Variable pressure single crystal X-ray diffraction: cell parameters (* denotes laboratory measurement).

P / GPa	a / Å	sigma (a) / Å	b / Å	sigma (b) / Å	c / Å	sigma (c)	β / °	sigma (β) / °	V / Å^3	sigma (V) / Å^3	R(gt)
0*	15.247	4E-4	5.005	1E-4	10.4052	3E-4	131.936	1E-3	590.68	0.03	0.0247
0.137*	15.181	0.002	4.9938	2E-4	10.405	0.002	131.943	0.006	586.72	0.17	0.0555
0.68*	15.075	0.003	4.9857	0.0015	10.382	0.004	131.84	0.02	581.4	0.4	0.1151
1.12*	14.84	0.03	4.98	0.012	10.36	0.04	131.64	0.15	572	3	0.0678
2.01	14.67	0.02	4.946	0.003	10.365	0.011	131.97	0.05	559.1	1.1	0.0295
2.29	14.639	0.007	4.9393	5E-4	10.379	0.007	132.027	0.013	557.5	0.5	0.0558
2.95	14.477	0.006	4.9154	5E-4	10.425	0.007	132.46	0.013	547.3	0.4	0.0397
3.43	14.342	0.013	4.8946	0.0011	10.487	0.014	133.01	0.03	538.3	0.9	0.0443
4.03	14.231	0.009	4.856	6E-4	10.642	0.009	134.234	0.018	526.9	0.6	0.0425
4.41	14.168	0.008	4.8351	6E-4	10.715	0.008	134.825	0.018	520.6	0.5	0.036
4.66	14.126	0.008	4.8218	6E-4	10.753	0.008	135.162	0.018	516.4	0.5	0.0454
4.82	14.095	0.008	4.8107	0.005	10.788	0.008	135.458	0.018	513.1	0.5	0.0604
5.52	14.024	0.008	4.789	6E-4	10.837	0.008	135.927	0.019	506.3	0.5	0.0409

Table S4. Variable temperature single crystal X-ray diffraction: cell parameters (* denotes that the original monoclinic cell setting, in which the structure was solved, differed from that shown and was subsequently transformed using the matrix [1 0 -1 0 -1 0 0 0 -1].

T / K	a / Å	sigma (a) / Å	b / Å	sigma (b) / Å	c / Å	sigma (c)	β / °	sigma (β) / °	V / Å^3	sigma (V) / Å^3	R(gt)
120	15.21	0.002	5.0011	2E-4	10.4146	0.0013	131.89	0.02	589.8	0.2	2.95
130	15.214	0.002	5.0026	3E-4	10.4148	0.0014	131.9	0.02	590	0.3	2.89
140	15.2073	0.0017	5.004	2E-4	10.4088	0.0011	131.901	0.019	589.6	0.2	2.96
150	15.2141	0.005	5.00244	1.8E-4	10.414	1E-3	131.903	0.0016	589.9	0.17	3.06
160	15.2231	0.0016	5.00381	1.9E-4	10.4203	1E-3	131.921	0.017	590.61	0.17	3.02
170	15.2217	0.0014	5.00249	1.7E-4	10.4183	1E-3	131.908	0.016	590.4	0.16	3.14
180*	15.218	0.002	5.00361	1.7E-4	10.416	0.002	131.91	0.02	590.3	0.2	3.08
190	15.2174	0.0011	5.00308	1.4E-4	10.4141	8E-4	131.916	0.12	589.99	0.13	3.15
200	15.2245	0.0013	5.00333	1.6E-4	10.4168	9E-4	131.929	0.015	590.33	0.16	3.2
210	15.2264	0.0012	5.0031	1.5E-4	10.4178	8E-4	131.932	0.014	590.41	0.14	3.12
220*	15.228	0.004	5.0042	2E-4	10.419	0.003	131.91	0.03	590.8	0.4	3.1
230*	15.232	0.002	5.00486	1.7E-4	10.422	0.002	131.93	0.02	591.1	0.2	3.24
240*	15.2385	0.0017	5.00507	1.8E-4	10.422	0.002	131.94	0.02	591.2	0.2	3.2
250	15.249	0.004	5.0096	5E-4	10.429	0.003	132	0.05	592.1	0.5	3.3
260*	15.241	0.002	5.0051	1.4E-4	10.4228	0.0017	131.957	0.017	591.2	0.2	4.35
270*	15.245	0.005	5.0046	3E-4	10.427	0.004	131.93	0.04	591.8	0.5	3.24
280	15.256	0.005	5.009	6E-4	10.418	0.004	131.99	0.06	591.7	0.6	3.245
290	15.257	0.002	5.0084	3E-4	10.4251	0.0016	131.97	0.03	592.3	0.3	3.35
310	15.2554	0.0017	5.0076	2E-4	10.4222	0.0011	131.963	0.018	592	0.2	3.13
330	15.2629	0.0013	5.00948	1.5E-4	10.4271	9E-4	131.971	0.014	592.74	0.15	3.33
350	15.2693	0.0019	5.0086	2E-4	10.43	0.0013	131.98	0.02	592.9	0.2	3.21
370	15.2797	0.0017	5.00803	1.9E-4	10.4364	0.0012	132.036	0.019	593.14	0.1	3.28
380*	15.305	0.01	5.0165	8E-4	10.452	0.008	132.03	0.08	596	1	3.1
390	15.293	0.003	5.0111	0.003	10.4453	0.0018	132.05	0.03	594.4	0.3	3.35
400	15.303	0.006	5.0187	0.009	10.453	0.004	132.01	0.06	596.5	0.7	3.15
410*	15.305	0.008	5.0133	4E-4	10.447	0.007	132.08	0.07	595	0.8	3.36
420*	15.322	0.012	5.0199	1E-3	10.455	0.011	132.04	0.11	597.2	1.3	3.32
430*	15.286	0.007	5.0121	4E-4	10.432	0.006	132.05	0.05	593.5	0.6	3.57
440*	15.306	0.012	5.0145	1E-3	10.444	0.01	132	0.1	595.7	1.2	3.44
450	15.337	0.009	5.0246	0.0011	10.465	0.006	132.07	0.09	598.7	0.1	3.68
460*	15.321	0.012	5.0166	0.0011	10.447	0.011	132.01	0.1	596.6	1.2	3.59
470*	15.339	0.018	5.0221	0.0013	10.453	0.016	132.13	0.15	597.2	1.9	3.83
480*	15.348	0.013	5.0188	0.0011	10.45	0.012	132.04	0.11	597.8	1.4	4.07
490	15.356	0.014	5.047	0.002	10.454	0.012	132.05	0.17	601.6	1.8	7.48

Notes and references

1. S. A. Moggach, D. R. Allan, S. Parsons, and J. E. Warren, *J. Appl. Crystallogr.*, 2008, **41**, 249–251.
2. G. J. Piermarini, S. Block, J. D. Barnett, and R. A. Forman, *J. Appl. Phys.*, 1975, **46**, 2774–2780.
3. G. M. Sheldrick, *Acta Crystallogr. Sect. A Found. Crystallogr.*, 2008, **64**, 112–22.
4. P. W. Betteridge, J. R. Carruthers, R. I. Cooper, K. Prout, and D. J. Watkin, *J. Appl. Crystallogr.*, 2003, **36**, 1487–1487.
5. A. Dawson, D. R. Allan, S. Parsons, and M. Ruf, *J. Appl. Crystallogr.*, 2004, **37**, 410–416.
6. *SAINT*, Bruker-Nonius, Bruker-AXS, Madison, Wisconsin, USA, 2006.
7. S. Parsons, *SHADE*, 2004.
8. *XPREP*, Bruker-Nonius, Bruker-AXS, Madison, Wisconsin, USA, 2004.
9. *CrysAlis CCD, CrysAlis RED and associated programs, Oxford Diffraction Ltd., Abingdon, U.K.*, 2006.
10. O. V. Dolomanov, L. J. Bourhis, R. J. Gildea, J. A. K. Howard, and H. Puschmann, *J. Appl. Crystallogr.*, 2009, **42**, 339–341.
11. A. B. Cairns and A. L. Goodwin, *Phys. Chem. Chem. Phys.*, 2015, **17**, 20449–20465.
12. M. J. Cliffe and A. L. Goodwin, *J. Appl. Crystallogr.*, 2012, **45**, 1321–1329.